

Highly anisotropic transient optical response of charge density wave order in ZrTe₃Li Yue ^{1,*}, Amrit Raj Pokharel ², Jure Demsar ², Sijie Zhang,¹ Yuan Li,¹ Tao Dong,¹ and Nanlin Wang ^{1,3,†}¹*International Center for Quantum Materials, School of Physics, Peking University, Beijing 100871, China*²*Institute of Physics, Johannes Gutenberg University, 55128 Mainz, Germany*³*Beijing Academy of Quantum Information Sciences, Beijing 100913, China*

(Received 26 December 2022; accepted 29 March 2023; published 7 April 2023)

Low dimensionality in charge density wave (CDW) systems leads to anisotropic optical properties, in both equilibrium and nonequilibrium conditions. Here, we perform polarized two-color pump probe measurements on a quasi-one-dimensional material ZrTe₃, in order to study the anisotropic transient optical response in the CDW state. Profound in-plane anisotropy is observed with respect to the polarization of probe photons. Below T_{CDW} both the quasiparticle relaxation signal and amplitude mode (AM) oscillation signal are much larger, with \mathbf{E}_{pr} nearly parallel to the a axis ($\mathbf{E}_{\text{pr}} \parallel a$) than for \mathbf{E}_{pr} parallel to the b axis ($\mathbf{E}_{\text{pr}} \parallel b$). This reveals that the $\mathbf{E}_{\text{pr}} \parallel a$ signal provides much a larger response to the variation of the CDW gap. Interestingly, the lifetime of the AM oscillations observed with $\mathbf{E}_{\text{pr}} \parallel b$ is longer than $\mathbf{E}_{\text{pr}} \parallel a$. Moreover, at high pump fluence where the electronic order melts and the AM oscillations vanish for $\mathbf{E}_{\text{pr}} \parallel a$, the AM oscillatory response still persists for $\mathbf{E}_{\text{pr}} \parallel b$. We discuss the possible origins that lead to such an unusual discrepancy between the two polarizations.

DOI: [10.1103/PhysRevB.107.165115](https://doi.org/10.1103/PhysRevB.107.165115)**I. INTRODUCTION**

Low dimensionality plays a key role for the formation of charge density waves (CDWs). CDWs usually appear in quasi-one-dimensional (1D) or quasi-two-dimensional (2D) materials [1,2], where the low-dimensional electronic structure supports good Fermi-surface nesting. The electronic susceptibility, especially for quasi-1D systems, tends to diverge at the nesting wave vector $2\mathbf{k}_F$ [3,4], resulting in electronic instability and periodic modulation of the conducting electrons. Another important factor for CDW formation is electron-phonon coupling. At $2\mathbf{k}_F$, phonon modes tend to soften, leading to a new periodic modulation of the lattice structure [3–6].

A typical experimental characterization of the CDW phase is the measurement of optical properties, in both equilibrium and nonequilibrium conditions. Optical conductivity spectroscopy is a powerful tool to identify the single-particle gap in the CDW state, where a profound spectral weight redistribution happens in the low-energy range [7–10]. CDWs also induce new collective excitations consisting of amplitude (AM) and phase modes. The AM excitations involve ionic displacement around the periodically distorted atomic displacements, and can be observed in Raman spectroscopy as a soft optical mode with A_{1g} symmetry [11,12]. Besides these time-averaging spectroscopies which detect equilibrium properties, ultrafast pump probe techniques have been widely utilized to study the nonequilibrium dynamical evolution of the system after optical excitation [7–10,13–15]. The single-particle gap opening and the appearance of col-

lective AM are manifested in the time-domain spectra as changes in quasiparticle (QP) relaxation signals and coherent oscillations, respectively. Moreover, time-resolved probes can provide much more information of the system that is inaccessible in the equilibrium state, including nonthermal ultrafast phase transitions driven by pump excitation [16,17], and selective detection of the order parameter components during the relaxation process [16,18].

The low dimensionality of CDW systems can lead to strongly anisotropic optical responses. Optical conductivity experiments have built a thorough understanding of the anisotropy in the equilibrium state. For in-plane optical conductivities of many quasi-1D CDW systems, the gap signature mainly appears with the polarization direction along the in-plane projection of the $2\mathbf{k}_F$ vector (which is often the structural chain direction) [7,19]. In contrast, for the nonequilibrium dynamical relaxation process, the anisotropy of the transient optical response was seldom studied. Such studies would be meaningful for clarifying the dynamical evolution of the CDW state, and expand the understanding of cooperative phenomena. Here, we report polarized femtosecond pump probe measurements on a prototypical quasi-1D CDW material ZrTe₃. Our data reveal interesting and pronounced anisotropic transient optical responses of the system.

II. EXPERIMENTAL RESULTS

ZrTe₃ is a quasi-1D CDW metal with $T_{\text{CDW}} = 63$ K. It belongs to the space group $P2_1/m$, with $a = 5.89$ Å, $b = 3.93$ Å, $c = 10.09$ Å, $\beta = 97.8^\circ$, and $\alpha = \gamma = 90^\circ$ [11,20]. The structure consists of prisms stacking along the b axis. The sample has a stripe-like ab surface, with the long edge parallel to the b axis and the short edge parallel to the a axis. The ordering wave vector $\mathbf{q}_{\text{CDW}} = (0.07\mathbf{a}^*, 0, 0.33\mathbf{c}^*)$ corresponds

*lilyyue@pku.edu.cn

†nlwang@pku.edu.cn

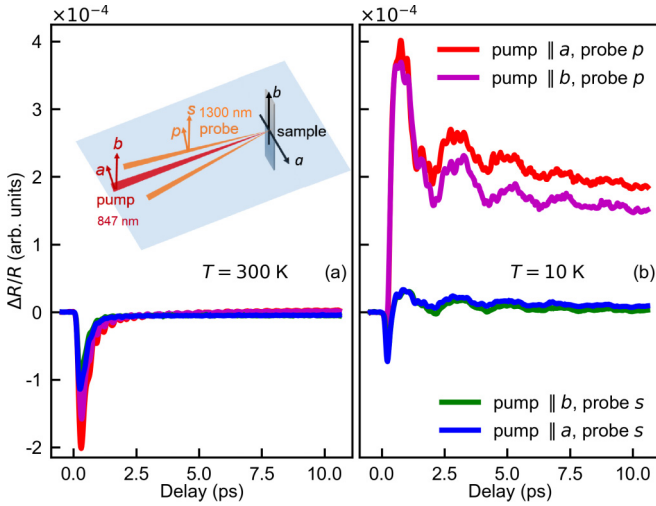


FIG. 1. (a) and (b) Time-resolved reflectivity under different polarization conditions at room temperature and 10 K, respectively, with pump fluence $\sim 60 \mu\text{J}/\text{cm}^2$. The inset of (a) depicts the reflection geometry of the experiment, where the a axis lies in the horizontal plane of incidence, and the b axis is along the vertical direction.

to the nesting of quasi-1D Fermi sheets near the Brillouin zone boundary [11,21,22]. Unlike other quasi-1D CDW materials such as NbSe_3 , $\text{K}_{0.3}\text{MoO}_3$, etc., \mathbf{q}_{CDW} is perpendicular to the structural chain direction. According to angle-resolved photoemission spectroscopy (ARPES) experiments, the quasi-1D Fermi sheets are partially gapped around the Brillouin zone D point [21,23], where the electron-phonon interaction is strongest [11]. Optical conductivity measurements showed an anisotropic gap feature which is more prominent along the in-plane a direction [24], with a depletion of spectral weights below 1000 cm^{-1} .

We performed two-color pump probe reflection measurements on the ab surface of ZrTe_3 single crystal [25]. Figure 1 displays the polarization-dependent transient reflectivity changes at room temperature and at 10 K. It is clear that the polarization of the probe photons makes a major difference in the signal amplitudes. In the CDW state [Fig. 1(b)], the difference between the two probe polarizations is much more profound than in the normal state [Fig. 1(a)]. Since the polarization-dependent spectra are dominated by the \mathbf{E}_{pr} direction, we focus on the results obtained with $\mathbf{E}_{\text{pr}} \parallel a$. Considering the rather small incident angle of the probe beam, the s and p polarizations can be approximated as nearly parallel to the b ($\mathbf{E}_{\text{pr}} \parallel b$) and a ($\mathbf{E}_{\text{pr}} \parallel a$) axis.

Figures 2(a) and 2(b) present the temperature evolution of the transient reflectivity change with $\mathbf{E}_{\text{pr}} \parallel a$ and $\mathbf{E}_{\text{pr}} \parallel b$, respectively. In Fig. 2(a), at 300 K the relaxation dynamics is given by a fast decaying negative signal with a small long-lived background signal extending far over the 10 ps time window. As temperature is decreased towards T_{CDW} , the long-lived background signal changes sign. Across the CDW transition, a second exponential decay process with a positive sign and longer relaxation time becomes apparent while the amplitude of the long-lived background response rapidly increases with decreasing temperature. Upon cooling to the

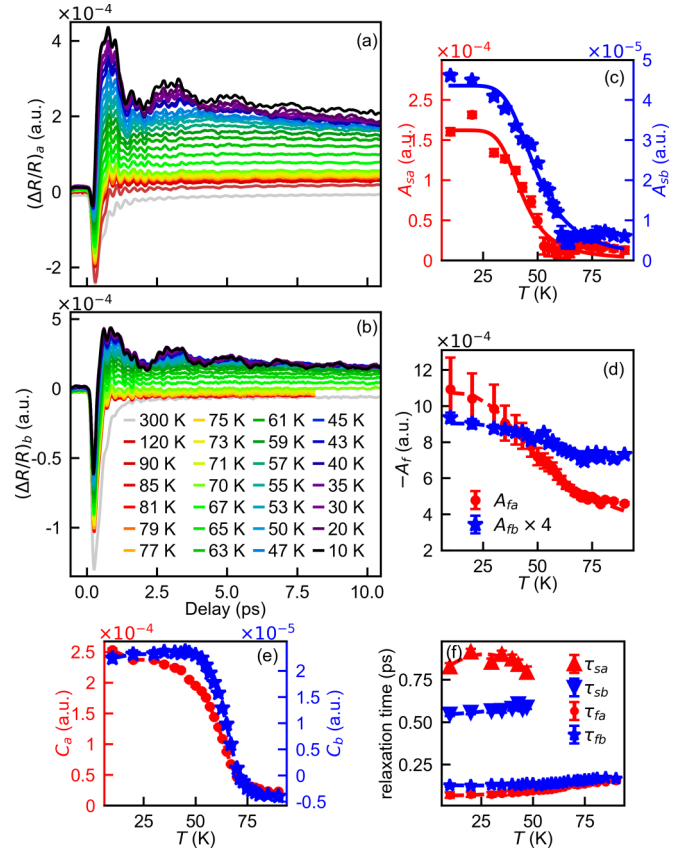


FIG. 2. (a) and (b) $\Delta R/R$ as a function of time delay at different temperatures for $\mathbf{E}_{\text{pr}} \parallel a$ and $\mathbf{E}_{\text{pr}} \parallel b$, with pump fluence $\sim 60 \mu\text{J}/\text{cm}^2$. (c)–(f) Temperature dependence of several parameters characterizing the QP relaxation dynamics. The red and blue markers correspond to spectra obtained with $\mathbf{E}_{\text{pr}} \parallel a$ and $\mathbf{E}_{\text{pr}} \parallel b$, respectively. The solid lines in (c) are the fitted curves with the RT model using T -independent gap [26]. The dashed lines are guides to the eye.

lowest temperature, the two exponentially decaying signals, as well as the long-lived signal, are further enhanced, and the oscillatory response due to the CDW amplitude mode with ~ 2 ps period becomes apparent. The spectra for $\mathbf{E}_{\text{pr}} \parallel b$ [Fig. 2(b)] show a similar trend, but with substantially lower signal amplitudes.

The QP relaxation dynamics can be fit by a convolution of a Gaussian response function and the following model function,

$$\left(\frac{\Delta R}{R}\right)_i = A_{fi} e^{-\frac{t}{\tau_{fi}}} + A_{si} e^{-\frac{t}{\tau_{si}}} + B_i t + C_i. \quad (1)$$

Here, $i = a$ or b denote the \mathbf{E}_{pr} polarization, A_{fi} and τ_{fi} are the amplitude and relaxation time of the fast negative exponential decay seen at all temperatures, and A_{si} and τ_{si} are the amplitude and relaxation time of the picosecond positive component arising in the CDW phase. The long-lived background signal should, in principle, be fitted with a third exponential decay with a very long relaxation time. However, since we are focusing on the short time dynamics on timescales of about 10 ps, we approximate the long-lived response by $B_i t + C_i$.

In the pump probe experiment, the pump pulse injects QPs into the system. If a gap opens near the Fermi level, photogen-

erated carriers will accumulate above the gap, the presence of the latter resulting in a relaxation bottleneck slowing down the relaxation process. The relaxation amplitude A_s at different temperatures can be described with the Rothwarf-Taylor (RT) model $A_s = \frac{E_I/\Delta_s}{1+\gamma \exp(-\Delta_s/k_B T)}$ [26], where E_I is the excitation density, γ is a fitting parameter, and Δ_s is the gap parameter which should be temperature independent in ZrTe₃ according to previous ARPES measurements [21]. Furthermore, in ZrTe₃, only parts of the Fermi surface are gapped by the CDW formation [21]. Therefore, part of the photogenerated carriers may rapidly relax to the ungapped region of the Fermi surface and relax via the normal electron-phonon thermalization process. The two exponentially decaying components in Eq. (1), with the faster one being present at all temperatures, likely stem from the two relaxation channels.

The amplitudes of both exponentially decaying components exhibit anomalies near T_{CDW} . In Fig. 2(c), A_{si} is nearly zero at high temperatures, and increases rapidly below T_{CDW} . A_{fi} are also enhanced in the CDW state [Fig. 2(d)], however, they remain pronounced far above T_{CDW} . Compared to the value at 10 K, A_{fi} above T_{CDW} is about 40% of its low-temperature value for $\mathbf{E}_{pr} \parallel a$ and 80% for $\mathbf{E}_{pr} \parallel b$, consistent with the assignment of the fast decay component to the normal relaxation processes in the ungapped regions. The relaxation times τ_{fi} are on the order of ~ 100 fs, displaying no anomalies near T_{CDW} , consistent with this scenario. The long-lived signal C_i also changes dramatically near T_{CDW} . This signal may be in part related to the bolometric response as well as to the localized in-gap carriers [13,14], whose contribution is reduced above T_{CDW} , consistent with the pronounced drop in C_i at temperatures above T_{CDW} .

Previously, the anisotropic optical response to the CDW gap formation was mainly studied by optical conductivity measurement of the equilibrium state. Here, in quasi-1D systems, the electronic structures are highly anisotropic. The Fermi-surface nesting happens between parts of anisotropic Fermi surfaces which are highly dispersing along the direction of the nesting vector \mathbf{q}_{CDW} and weakly dispersing along the direction perpendicular to \mathbf{q}_{CDW} . When the nested parts of Fermi surfaces are gapped out, the density of free carriers is strongly reduced, and the gap feature in the equilibrium optical conductivity is more prominent along the Fermi nesting direction and is weak along the perpendicular direction. The gap feature is observed in the low-frequency range, at energy comparable to the CDW gap. In the near-infrared range, far above the CDW gap, the changes in optical conductivity induced by the CDW transition are very weak and are usually not resolved in the equilibrium spectra.

In the optical pump probe experiment, however, owing to the high sensitivity of the technique (here, small modulations of the order of 10^{-5} can be routinely measured, while the accuracy of the equilibrium spectroscopy is of the order of 10^{-2}), one can measure the transient reflectivity changes in the near-infrared range caused by the pump-induced gap suppression and subsequent carrier relaxation. Our polarized pump probe study, even at 0.95 eV (1300 nm) probe photon energy, clearly demonstrates a profound anisotropic transient optical response in the CDW state, where the $\mathbf{E}_{pr} \parallel a$ signal in the CDW state is about an order of magnitude larger than

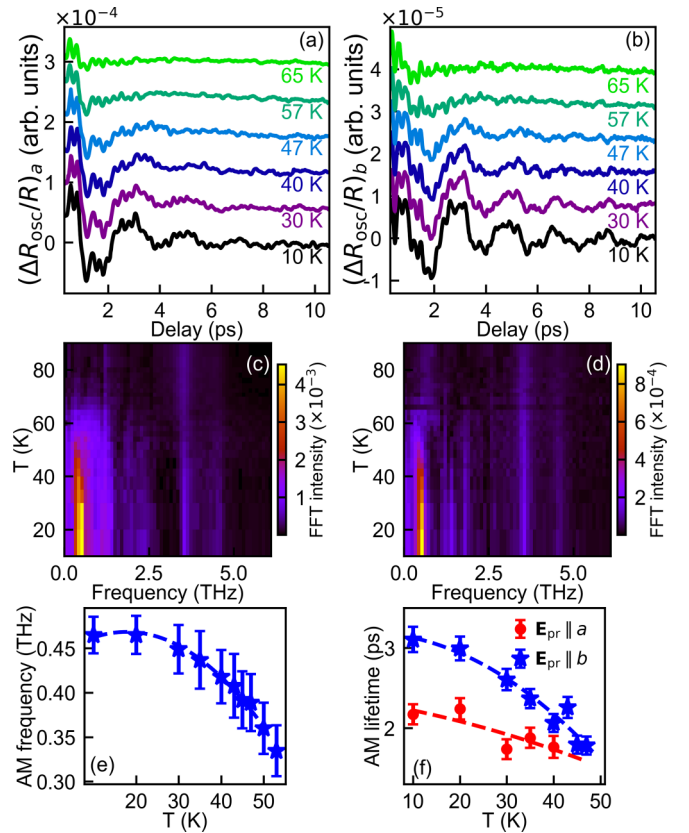


FIG. 3. (a) and (b) The oscillation part of transient reflectivity change for $\mathbf{E}_{pr} \parallel a$ and $\mathbf{E}_{pr} \parallel b$, with pump fluence $\sim 60 \mu\text{J}/\text{cm}^2$. Lines are vertically shifted for clarity. (c) and (d) correspond to the fast Fourier transformation of the oscillation part for $\mathbf{E}_{pr} \parallel a$ and $\mathbf{E}_{pr} \parallel b$, respectively. (e) The temperature dependence of the AM peak frequency obtained by fitting the peak position in the FFT spectra of (d). (f) The lifetime of AM oscillation for different probe photon polarizations, obtained by fitting the time-domain oscillation.

for $\mathbf{E}_{pr} \parallel b$. At temperatures above T_{CDW} , however, the difference between the responses in the two probe polarizations is quite small [see Figs. 1(a) and 2(d)]. We note that such an anisotropy of the response in the CDW state should not be taken for granted in quasi-1D CDW systems. For example, in studies of $\text{K}_{0.3}\text{MoO}_3$, the anisotropy between the probe polarizations along the chain or perpendicular to the chain directions is quite weak (see the Supplemental Material in Ref. [18]).

Figures 3(a) and 3(b) display the oscillatory component of the spectra along two polarizations, obtained by subtracting the fitted QP relaxation curve of Eq. (1) from the raw traces in Figs. 2(a) and 2(b). Figures 3(c) and 3(d) present the corresponding fast Fourier transformation (FFT). Several distinct modes are observed at around 0.47, 1.74, 3.5, 4.5, and 6.55 THz, among which the 0.47 THz mode, disappearing above T_{CDW} , shows clear signatures of the amplitude mode. As the temperature rises, the AM intensity decays and the mode softens [Fig. 3(e)], consistent with the Raman measurements [11]. Comparing the two polarizations, the AM oscillation intensity for $\mathbf{E}_{pr} \parallel a$ is much stronger than that for $\mathbf{E}_{pr} \parallel b$. The highly

anisotropic AM intensity was also reported in a quasi-1D CDW material $(\text{TaSe}_4)_2\text{I}$, where the AM mode shows up only with the probe photon polarized along the CDW axis [27]. Since the AM collective dynamics involves the oscillation of the CDW gap [17,28], the larger AM amplitude for $\mathbf{E}_{\text{pr}} \parallel a$ implies that $\mathbf{E}_{\text{pr}} \parallel a$ provides a much larger response to the photoinduced variation of the CDW gap. This is consistent with the larger QP relaxation signal for the probe polarized along the a axis due to the gap formation below T_{CDW} , as discussed in the preceding section.

The oscillatory AM signal can be described with a damped oscillator

$$\frac{\Delta R_{\text{osc}}}{R}(t) = A_{\text{AM}} e^{-t/\tau_{\text{AM}}} \sin(\omega_{\text{AM}} t + \phi), \quad (2)$$

where A_{AM} , τ_{AM} , ω_{AM} , and ϕ correspond to the amplitude, lifetime, frequency, and phase. An interesting result of our measurements is that the AM lifetime also exhibits anisotropy [see Fig. 3(f)]: The lifetime is shorter for $\mathbf{E}_{\text{pr}} \parallel a$ than for $\mathbf{E}_{\text{pr}} \parallel b$. This difference can also be directly seen in the time-domain traces, where the oscillations in Fig. 3(b) extend longer than in Fig. 3(a). We discuss the possible origins of this observation later.

We also studied the pump fluence dependence of the dynamics at 10 K [Figs. 4(a) and 4(b)]. By increasing the pump fluence, the system will go from a linear, weak perturbation regime to quenching the CDW state. This has been observed in other CDW materials, showing that strong perturbation leads to an ultrafast melting of the electronic order where the gap is closed and the AM amplitudes saturate and eventually vanish [16,17]. In ZrTe_3 , with increasing fluence, the fast negative exponential increases monotonically, but becomes less anisotropic, as expected from the T -dependence measurements. The slower positive exponentially decaying component, which corresponds to the QP relaxation across the CDW gap, also grows linearly at first but then fades away [Fig. 4(b) inset]. Such changes of QP relaxation signals are consistent with ultrafast melting of the electronic order. At high pump fluence, a broad hump appears on the higher-frequency side of the AM peak in the FFT spectra, which may be related to enhanced anharmonicity under strong perturbation. Along with the melting of electronic order, the AM oscillation gradually vanishes for $\mathbf{E}_{\text{pr}} \parallel a$ [Figs. 4(c) and 4(f)]. Interestingly, for $\mathbf{E}_{\text{pr}} \parallel b$ the AM oscillation exists up to the highest fluences [Figs. 4(d) and 4(g)].

Generally, one would expect the amplitude mode to saturate and subsequently disappear as the electronic order is melted by high fluence, regardless of the probe photon polarization. Yet here, the AM oscillation for $\mathbf{E}_{\text{pr}} \parallel b$ survives to the highest fluence, with its amplitude and lifetime nearly independent on fluence above $\sim 100 \mu\text{J}/\text{cm}^2$ [Fig. 4(e)]. In the following we discuss the possible origins that may be responsible for the different fluence dependences of the AM amplitudes between two probe polarizations, as well as the different lifetimes shown in Fig. 3(f).

III. DISCUSSION

First, given the nonlinearity of the AM response, we consider the influence of the mismatch between penetration depths. The optical penetration depths are determined from

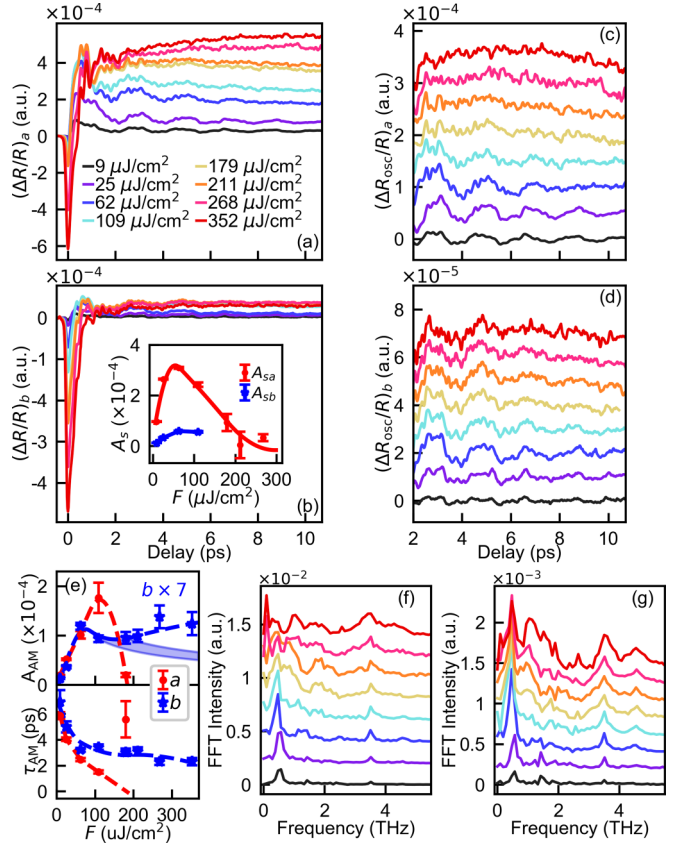


FIG. 4. (a) and (b) The transient reflectivity change at different pump fluences at 10 K, with $\mathbf{E}_{\text{pr}} \parallel a$ and $\mathbf{E}_{\text{pr}} \parallel b$, respectively. The inset of (b) shows the amplitude of the slower positive exponential at different fluences. For $\mathbf{E}_{\text{pr}} \parallel b$ we can only obtain a reasonable fitting parameter $A_{s,b}$ below $179 \mu\text{J}/\text{cm}^2$. (c) and (d) The oscillation part of the time-domain spectra of (a) and (b), obtained by subtracting the fitted QP relaxation curve of from the raw traces in (a) and (b). Data are taken from 2 ps to avoid the residual quasiparticle relaxation signal which is not perfectly subtracted. (e) The fluence dependence of the amplitude (upper panel) and lifetime (lower panel) of the AM oscillation, obtained by fitting the time-domain oscillation spectra with Eq. (2). Details about the fitting procedure are shown in the Supplemental Material [25]. The shaded region in the upper panel expected intensity range in the condition that the existence of the AM signal at high fluence with $\mathbf{E}_{\text{pr}} \parallel b$ is purely induced by the mismatch of penetration depth [25]. (f) and (g) The fast Fourier transformation of the time-domain oscillation signal for different probe polarizations.

the reported reflectivity data by Herr *et al.* [29], using a Kramers-Kronig analysis [30]. The penetration depth at the 1300 nm probe wavelength is 28.2 nm for $\mathbf{E}_{\text{pr}} \parallel a$ and 89.2 nm for $\mathbf{E}_{\text{pr}} \parallel b$ while at the 847 nm pump wavelength it is 22.5 nm for $\mathbf{E}_{\text{pu}} \parallel a$ and 47.8 nm for $\mathbf{E}_{\text{pu}} \parallel b$.

The large mismatch can thus be responsible for different fluence dependences of the AM signal. Let us first consider the fluence dependence of the response for the case, where pump and probe mismatch is negligible, or when the optical penetration depth is larger than that of the probe. For weak perturbations, the amplitude of the AM signal is usually linearly proportional with the pump fluence. Above

the absorbed energy density corresponding to quenching the electronic order, however, the signal will saturate [16] and eventually disappear. Indeed, this scenario well accounts for our observations with $\mathbf{E}_{\text{pr}} \parallel a$. For the case where the pump penetration depth is shorter than the probe penetration depth, i.e., for $\mathbf{E}_{\text{pr}} \parallel b$, however, the situation is more complicated. Beyond the linear response regime, the high incident pump fluence results in quenching of the electronic order in the surface layer given by the pump penetration depth. However, for the deeper regions (still probed by the probe), the absorbed energy density is still below the CDW melting threshold, resulting in a contribution to the reflectivity transient of the perturbed CDW state. Indeed, our observations with $\mathbf{E}_{\text{pr}} \parallel b$ are qualitatively consistent with this scenario. For example, the quenched surface region may be responsible for the broad hump feature and broadened phonon peaks in the FFT spectra, with the deeper, weakly perturbed regions giving rise to the AM response far beyond the threshold seen in the $\mathbf{E}_{\text{pr}} \parallel b$ experiment.

In order to check this scenario, we performed a quantitative analysis with the above model, presented in the Supplemental Material [25]. The model, taking into account the optical penetration length mismatch, is qualitatively consistent with our experimental observations. However, after quenching of the electronic order in the surface layer, by further increasing the pump fluence, the volume fraction of the quenched CDW state will increase, leading to a decrease of the AM signal intensity. According to the model, the AM signal intensity should drop faster with increasing fluence as compared to our experimental results. The predicted dependence of the amplitude of the AM is given by the dashed blue region in Fig. 4(e) [25], showing that for fluences beyond $\approx 100 \mu\text{J}/\text{cm}^2$, the AM signal intensity for $\mathbf{E}_{\text{pr}} \parallel b$ should start to decay. However, the measured AM signal intensity for $\mathbf{E}_{\text{pr}} \parallel b$ is nearly constant and may even be increasing with increasing pump fluence. Moreover, we note that the lifetimes of the AM oscillations in Fig. 1(b) do not change much when switching the pump polarization to from the a to b direction (Supplemental Fig. 2) [25], even though the difference in the pump penetration depths is about a factor of two. Thus, the penetration depth mismatch may not be solely responsible for our observations. We should note, however, that the nonlinearity of the AM signal can be more complicated than our simple phenomenological analysis. Also, the damped oscillator function may not be an accurate model describing the AM behavior under nonlinear conditions.

Given that the penetration mismatch can only resolve part of the observed anisotropy of the AM response, next we discuss an alternative scenario that may also (or in addition) be responsible for the anisotropic fluence-dependent AM response. We first note that the CDW order parameter comprises electronic and lattice parts, and the amplitude mode involves oscillation of the electronic gap [17,28,31] and the periodic lattice displacements [32]. Usually, the two parts are considered to be adiabatically coupled due to electron-phonon coupling. However, at least on timescales shorter than the AM period, this assumption may be invalid [15,18]. First, in earlier studies, different techniques have been utilized to probe the ultrafast dynamics of the two components of the CDW order. In TbTe_3 , time-resolved photoemission demonstrated the

oscillation of the CDW gap at the ~ 2.4 THz AM frequency [17,28]. Above $\sim 1 \text{ mJ}/\text{cm}^2$, the gap is closed by strong excitation and the AM oscillation is no longer resolved. However, the time-resolved x-ray diffraction study on TbTe_3 showed that with $3 \text{ mJ}/\text{cm}^2$ fluence the superlattice peak intensity still oscillates at the AM frequency [32]. In $\text{K}_{0.3}\text{MoO}_3$, x-ray studies suggest a critical fluence of $1 \text{ mJ}/\text{cm}^2$ for the collapse of the superlattice [33], but an optical reflectivity probe showed a critical fluence of $\sim 0.3 \text{ mJ}/\text{cm}^2$, where damping and disappearance of the AM oscillation is observed [16]. Finally, at fluences much higher than those needed to collapse the electronic order, a collapse and revival of the periodic lattice modulation has been observed [33,34]. Thus, it can be inferred that the nonequilibrium dynamics of the electronic and lattice subsystems are not always strictly entangled [35]. Under strong perturbation, the electronic order is melted and the CDW band oscillation vanishes (or become too small to detect), but the lattice part may still display well-resolved oscillatory dynamics. Such a disentangled dynamics may be responsible for the observed anisotropy in the fluence dependence of AM in ZrTe_3 , as discussed below.

To describe this scenario, we first point out that transient reflectivity probes both the CDW gap and lattice components of the dynamical AM response, with different weights. The weights may depend on the photon energy. For example, if the probe frequency is close to the gap frequency, one is likely to see the gap oscillation directly, but, if the photon energy is near some interband transition at high energies, one can expect a larger contribution from the lattice component. It should be noted that the transient reflectivity does not directly detect the ion motion, so the lattice oscillation is probed due to its modulation of the interband transition, since the electronic band positions and intensities of folded electronic bands are oscillating along with driven atomic motion [15]. The weights may also depend on photon polarizations. Here, the quasi-1D system has a highly anisotropic electronic structure with large anisotropy in the dielectric function up to the visible range [29]. The anisotropic CDW gap affects the optical conductivities mainly along the a direction [24]. Given the large difference of the signal amplitudes between the two polarizations in response to the variation of the CDW gap in our transient reflectivity measurement, it is possible that coherent AM oscillations observed in the a and b polarizations are mainly related to the collective dynamics of the electronic and lattice subsystem, respectively.

Such a scenario is consistent with our observed fluence dependence of AM oscillation signals along the two probe polarizations. At high fluence, the disappearance of the AM signal for $\mathbf{E}_{\text{pr}} \parallel a$ corresponds to the strong suppression of the AM oscillations of the electronic gap, while the AM signal for $\mathbf{E}_{\text{pr}} \parallel b$ corresponds to the vibration of the lattice part disentangled from the electronic dynamics. This scenario may be realized in ZrTe_3 given the fact that $\mathbf{E}_{\text{pr}} \parallel a$ provides a much larger response to the variation of the CDW gap, as shown by the profound intensity of the quasiparticle relaxation and the AM oscillation signals in this polarization. For $\mathbf{E}_{\text{pr}} \parallel a$, the measured AM oscillation is dominated by the dynamical evolution of the CDW gap. For $\mathbf{E}_{\text{pr}} \parallel b$, the signal is weakly sensitive to the variation of the gap, as well as to the incoherent hot electron dynamics near the Fermi level, so instead

the response would be dominated by the lattice AM vibration. Indeed, such a scenario agrees with the different amplitudes of individual components to transient reflectivity in the two probe polarizations—see Fig. 1(b). Here, for $\mathbf{E}_{\text{pr}} \parallel a$, the QP exponential decay is very prominent, but for $\mathbf{E}_{\text{pr}} \parallel b$ the signal is dominated by the coherent AM oscillation.

IV. CONCLUSION

In summary, we use polarized femtosecond pump probe experiments to investigate the nonequilibrium dynamical optical response in ZrTe_3 . Profound anisotropy is observed with respect to the polarization of probe photons. With $\mathbf{E}_{\text{pr}} \parallel a$, the spectra present a much larger response to the formation of a CDW gap below T_{CDW} as well as to the variation of the CDW gap during AM oscillations. Interestingly, we observe that the AM oscillation signal presents different damping lifetime between $\mathbf{E}_{\text{pr}} \parallel a$ and $\mathbf{E}_{\text{pr}} \parallel b$. Moreover, the AM oscillation signal for $\mathbf{E}_{\text{pr}} \parallel b$ is seen to persist to a much higher pump fluence than for $\mathbf{E}_{\text{pr}} \parallel a$. While the results may be attributed

to the anisotropy of the pump and probe penetration depths, they may also be linked to the disentangled collective dynamics of electronic and lattice parts of the order parameter. Although numerous optical pump probe measurements have been performed on low-dimensional CDW materials, our results suggest that additional spectrally resolved studies may further our understanding of the cooperative phenomena in CDW materials as well as correlated materials in general.

ACKNOWLEDGMENTS

This work was supported by NSFC (No. 11888101) and National Key Research and Development Program of China (No. 2022YFA1403900). L.Y. further acknowledges support from China Postdoctoral Science Foundation (No. 2021M700257) and National Postdoctoral Program for Innovative Talents (No. BX20200016). A.R.P. and J.D. acknowledge support by the Deutsche Forschungsgemeinschaft (DFG, German Research Foundation) - TRR 288 - 422213477 (project B08).

-
- [1] P. Monceau, *Adv. Phys.* **61**, 325 (2012).
 [2] K. Rossnagel, *J. Phys.: Condens. Matter* **23**, 213001 (2011).
 [3] G. Grüner, *Density Waves in Solids* (CRC Press, Boca Raton, FL, 2018).
 [4] G. Grüner, *Rev. Mod. Phys.* **60**, 1129 (1988).
 [5] J. P. Pouget, B. Hennon, C. Escribe-Filippini, and M. Sato, *Phys. Rev. B* **43**, 8421 (1991).
 [6] M. Hoesch, A. Bosak, D. Chernyshov, H. Berger, and M. Krisch, *Phys. Rev. Lett.* **102**, 086402 (2009).
 [7] R. S. Li, L. Yue, Q. Wu, S. X. Xu, Q. M. Liu, Z. X. Wang, T. C. Hu, X. Y. Zhou, L. Y. Shi, S. J. Zhang, D. Wu, T. Dong, and N. L. Wang, *Phys. Rev. B* **105**, 115102 (2022).
 [8] T. Lin, L. Y. Shi, Z. X. Wang, S. J. Zhang, Q. M. Liu, T. C. Hu, T. Dong, D. Wu, and N. L. Wang, *Phys. Rev. B* **101**, 205112 (2020).
 [9] R. Y. Chen, B. F. Hu, T. Dong, and N. L. Wang, *Phys. Rev. B* **89**, 075114 (2014).
 [10] R. Y. Chen, S. J. Zhang, M. Y. Zhang, T. Dong, and N. L. Wang, *Phys. Rev. Lett.* **118**, 107402 (2017).
 [11] Y. Hu, F. Zheng, X. Ren, J. Feng, and Y. Li, *Phys. Rev. B* **91**, 144502 (2015).
 [12] C. S. Snow, J. F. Karpus, S. L. Cooper, T. E. Kidd, and T.-C. Chiang, *Phys. Rev. Lett.* **91**, 136402 (2003).
 [13] J. Demsar, K. Biljaković, and D. Mihailovic, *Phys. Rev. Lett.* **83**, 800 (1999).
 [14] J. Demsar, L. Forró, H. Berger, and D. Mihailovic, *Phys. Rev. B* **66**, 041101(R) (2002).
 [15] H. Schaefer, V. V. Kabanov, and J. Demsar, *Phys. Rev. B* **89**, 045106 (2014).
 [16] A. Tomeljak, H. Schäfer, D. Städter, M. Beyer, K. Biljakovic, and J. Demsar, *Phys. Rev. Lett.* **102**, 066404 (2009).
 [17] F. Schmitt, P. S. Kirchmann, U. Bovensiepen, R. G. Moore, L. Rettig, M. Krenz, J. H. Chu, N. Ru, L. Perfetti, D. H. Lu, M. Wolf, I. R. Fisher, and Z. X. Shen, *Science* **321**, 1649 (2008).
 [18] H. Schäfer, V. V. Kabanov, M. Beyer, K. Biljakovic, and J. Demsar, *Phys. Rev. Lett.* **105**, 066402 (2010).
 [19] A. Perucchi, L. Degiorgi, and R. E. Thorne, *Phys. Rev. B* **69**, 195114 (2004).
 [20] K. Stöwe and F. R. Wagner, *J. Solid State Chem.* **138**, 160 (1998).
 [21] T. Yokoya, T. Kiss, A. Chainani, S. Shin, and K. Yamaya, *Phys. Rev. B* **71**, 140504(R) (2005).
 [22] L. Yue, S. Xue, J. Li, W. Hu, A. Barbour, F. Zheng, L. Wang, J. Feng, S. B. Wilkins, C. Mazzoli, R. Comin, and Y. Li, *Nat. Commun.* **11**, 98 (2020).
 [23] M. Hoesch, L. Gannon, K. Shimada, B. J. Parrett, M. D. Watson, T. K. Kim, X. Zhu, and C. Petrovic, *Phys. Rev. Lett.* **122**, 017601 (2019).
 [24] A. Perucchi, L. Degiorgi, and H. Berger, *Eur. Phys. J. B* **48**, 489 (2005).
 [25] See Supplemental Material at <http://link.aps.org/supplemental/10.1103/PhysRevB.107.165115> for additional methods, measurement data, and analyses.
 [26] J. Demsar, B. Podobnik, V. V. Kabanov, T. Wolf, and D. Mihailovic, *Phys. Rev. Lett.* **82**, 4918 (1999).
 [27] W. Bronsch, M. Tuniz, G. Crupi, M. De Col, D. Puntel, D. Soranzio, A. Giammarino, M. Perlangeli, H. Berger, D. De Angelis, D. Fainozzi, E. Paltanin, J. S. Pelli Cresi, G. Kurdi, L. Foglia, R. Mincigrucci, F. Parmigiani, F. Bencivenga, and F. Cilento, *Faraday Discuss.* **237**, 40 (2022).
 [28] F. Schmitt, P. S. Kirchmann, U. Bovensiepen, R. G. Moore, J.-H. Chu, D. H. Lu, L. Rettig, M. Wolf, I. R. Fisher, and Z.-X. Shen, *New J. Phys.* **13**, 063022 (2011).
 [29] S. Herr and J. Brill, *Synth. Met.* **16**, 283 (1986).
 [30] The high-frequency optical conductivity spectra reported by Perucchi *et al.* in Ref. [24] show no difference between two polarizations. We have confirmed with the authors that this is because the high-frequency parts are measured without a polarizer.
 [31] P. E. Dolgirev, A. V. Rozhkov, A. Zong, A. Kogar, N. Gedik, and B. V. Fine, *Phys. Rev. B* **101**, 054203 (2020).
 [32] R. G. Moore, W. S. Lee, P. S. Kirchman, Y. D. Chuang, A. F. Kemper, M. Trigo, L. Patthey, D. H. Lu, O. Krupin, M. Yi,

- D. A. Reis, D. Doering, P. Denes, W. F. Schlotter, J. J. Turner, G. Hays, P. Hering, T. Benson, J.-H. Chu, T. P. Devereaux *et al.*, [Phys. Rev. B **93**, 024304 \(2016\)](#).
- [33] T. Huber, S. O. Mariager, A. Ferrer, H. Schäfer, J. A. Johnson, S. Grübel, A. Lübcke, L. Huber, T. Kubacka, C. Dornes, C. Laulhe, S. Ravy, G. Ingold, P. Beaud, J. Demsar, and S. L. Johnson, [Phys. Rev. Lett. **113**, 026401 \(2014\)](#).
- [34] M. J. Neugebauer, T. Huber, M. Savoini, E. Abreu, V. Esposito, M. Kubli, L. Rettig, E. Bothschafter, S. Grübel, T. Kubacka, J. Rittmann, G. Ingold, P. Beaud, D. Dominko, J. Demsar, and S. L. Johnson, [Phys. Rev. B **99**, 220302\(R\) \(2019\)](#).
- [35] Here, we also need to be careful that the different critical fluences may be a result of different penetration depths of the probe techniques. Usually, the penetration depths of x-ray photons are substantially longer than photons in the near-infrared range. But in these time-resolved x-ray diffraction experiments, grazing incidence geometry is used, so the mismatch between optical pump light and x rays is small.